

Surface Rhenium Oxide–Support Interaction for Supported Re_2O_7 Catalysts

DU SOUNG KIM¹ AND ISRAEL E. WACHS²

*Zettlemoyer Center for Surface Studies, Department of Chemical Engineering, Lehigh University,
Bethlehem, Pennsylvania 18015*

Received October 31, 1991; revised January 4, 1993

The molecular structures of the two-dimensional rhenium oxide overlayers on different oxide supports (Al_2O_3 , TiO_2 , ZrO_2 , SiO_2 , and MgO) under ambient and dehydrated conditions were determined by Raman spectroscopy. The surface rhenium oxide species under ambient conditions are hydrated by adsorbed moisture and are essentially in an aqueous medium. Consequently, the surface rhenium oxide species under ambient conditions resemble the ReO_4^- ion in an aqueous solution independent of the specific oxide support. Upon dehydration at elevated temperatures, the surface rhenium oxide species interact with the oxide support by a bridged oxygen (with exception of the $\text{Re}_2\text{O}_7/\text{MgO}$ system). The molecular structures of the dehydrated surface rhenium oxide species possess an isolated, four-coordinated rhenium oxide species with three terminal $\text{Re}=\text{O}$ bonds and one bridging $\text{Re}-\text{O}-\text{Support}$ bond. For the $\text{Re}_2\text{O}_7/\text{MgO}$ systems, the surface rhenium oxide species is primarily present as a compound(s) formed by a strong acid–base interaction between the deposited rhenium oxide and the magnesium oxide support. Methanol oxidation over the supported rhenium oxide catalysts revealed that the activity is strongly dependent on the specific oxide support and increases with increasing reducibility of the surface rhenium oxide species. The activity and reducibility of the supported rhenium oxide catalysts are attributed to the difference in the $\text{Re}^7-\text{O}-\text{support}$ bond strength. © 1993 Academic Press, Inc.

INTRODUCTION

Supported rhenium oxide catalysts are used extensively for metathesis of olefins (1, 2) and have been examined for hydrodesulfurization (HDS) of heavy fractions of crude oil (3, 4). It is well established that supported rhenium oxide catalysts exhibit a higher catalytic activity for these reactions than the corresponding supported molybdenum and tungsten oxide catalysts. To enhance the catalytic activity of $\text{Re}_2\text{O}_7/\text{Al}_2\text{O}_3$ for metathesis, other metal oxides (V_2O_5 , MoO_3 , or WO_3) are introduced to $\text{Re}_2\text{O}_7/\text{Al}_2\text{O}_3$ (5–7), as well as mixed oxide supports such as $\text{SiO}_2 \cdot \text{Al}_2\text{O}_3$, $\text{Al}_2\text{O}_3 \cdot \text{B}_2\text{O}_3$, and

$\text{Al}_2\text{O}_3 \cdot \text{AlPO}_4$ are used instead of the Al_2O_3 support (7–9). Moreover, the catalytic activity is further increased by the addition of MR_4 ($M = \text{Sn}$ or Pb , $R = \text{alkyl}$) to the supported rhenium oxide catalysts (10).

The industrial importance of rhenium-based catalysts has motivated a large number of studies to determine the surface structures of supported rhenium oxide catalysts by Fourier transform infrared (FTIR) (11–13), extended X-ray absorption fine structure (EXAFS) (14), X-ray absorption near edge structure (XANES) (14, 15), and Raman spectroscopy (12, 13, 15–17). The detailed structural information of supported rhenium oxide catalysts has been derived primarily from Raman spectroscopy studies because of the molecular nature of this characterization method and its ability to discriminate between different metal oxide

¹ Present address: Research and Development Division, Daelim Engineering Co. Ltd., #17-5, Yoido-dong, Youngdungpo-ku, Seoul, 150-010 Korea.

² To whom correspondence should be addressed.

species that may simultaneously be present in the catalyst.

Recently, Wachs *et al.* (18, 19) have demonstrated that the specific oxide support is a critical parameter since it dramatically affects the reactivity of the surface metal oxide species. They have also proposed that the reactivity for methanol oxidation is related to the bridging oxygen bond that interacts with the oxide support rather than terminal $M=O$ bond (18, 19). Several studies have shown recently that temperature-programmed reduction (TPR) is a characterization technique very effective in determining the interaction between surface metal oxides and the support. Arnoldy *et al.* (20) have proposed that differences in reducibility of Re_2O_7 on various oxide supports (Al_2O_3 , SiO_2 , and C) are due to differences in the strength of the Re^{7+} -support interaction and showed that the strength of the Re^{7+} -support interaction decreases in the order: $Al_2O_3 > SiO_2 > C$. Similarly, Vuurman *et al.* (13) have also revealed using TPR that the bridging $Re-O$ -support bond strength for Re_2O_7 /support catalysts is strongly dependent on the type of oxide support and decreases in the order: $Al_2O_3 > SiO_2 \geq ZrO_2 > TiO_2$.

Methanol oxidation is well known as a sensitive probe reaction (18, 21–25). The catalytic activity and selectivity for the methanol oxidation reaction are strongly dependent on the surface morphology of unsupported (21, 22) and supported metal oxide catalysts (18, 23–25). It is also used as a model reaction to characterize the surface properties of catalysts (23, 24) as well as the interaction between the deposited surface oxide and the oxide support (18, 25). Thus, the present study employs the methanol oxidation as a chemical probe to study the surface rhenium oxide-support interaction.

The molecular design of supported rhenium oxide catalysts requires a systematic investigation of the surface structures of rhenium oxide species on oxide supports as well as the surface rhenium oxide-support interaction and its influence on catalysis.

The present study focuses on the surface structure of rhenium oxide species on oxide supports and the influence of the resultant surface properties on the catalytic activity and selectivity for methanol oxidation (the probe reaction).

EXPERIMENTAL

Catalyst preparation. The support materials used in this study were Al_2O_3 (Harshaw, $180\text{ m}^2\text{ g}^{-1}$), TiO_2 (Degussa P-25, $55\text{ m}^2\text{ g}^{-1}$), ZrO_2 (Degussa, $39\text{ m}^2\text{ g}^{-1}$), and SiO_2 (Cab-O-Sil, $300\text{ m}^2\text{ g}^{-1}$). MgO ($80\text{ m}^2\text{ g}^{-1}$) was prepared by the dehydration of magnesium hydroxide [$Mg(OH)_2$, Fluka Chemical Co.] at 973 K for 2 h. The pH at point of zero charge (PZC) for Al_2O_3 , TiO_2 , ZrO_2 , SiO_2 , and MgO are 6.0–8.9, 6.2, 6.7, 3.1, and 12.4, respectively (26, 27). The 1% Re_2O_7 catalysts supported on the different metal oxide supports were prepared by an incipient wetness impregnation method with a 60–70 wt% aqueous solution of perrhenic acid, $HReO_4$ (Alfa) (14). After impregnation, the samples were dried at room temperature, dried at 373 K 16 h, and then calcined at 773 K for 16 h.

Raman spectroscopy. The Raman spectra of the 1% Re_2O_7 /support samples, under ambient and dehydrated conditions, were obtained with an Ar^+ ion laser (Spectra Physics Model 171) delivering about 15–40 mW of incident radiation. The excitation line of the Raman scattering was 514.5 nm. The scattered radiation from the sample was directed into a Spex Triplemate spectrometer (Model 1877) coupled to a Princeton Applied Research OMA III optical multichannel analyzer (Model 1463) equipped with an intensified photodiode array detector cooled thermoelectrically to 238 K. For the measurement of Raman spectra under ambient conditions, the samples were spun at ca. 2000 rpm to avoid laser-induced dehydration caused by local heating effects. A modified version of the *in situ* cell developed by Wang (12) was used for collecting the Raman spectra under dehydrated conditions. Prior to the *in situ* measurements, the

samples were dehydrated at 773 K for 1 h in flowing O_2 , and the Raman spectra of the dehydrated samples were subsequently collected at room temperature. Ultrahigh-purity, hydrocarbon-free oxygen (Linde gas) was purged through the cell during the acquisition of the Raman spectra.

Catalytic reactions. Partial oxidation of methanol was carried out at 503 K by using a fixed-bed tube reactor. Prior to the reaction, the catalyst was typically treated with flowing O_2 at 573 K for 1 h, and then the temperature was reduced to the reaction temperature. The reactor was held in a vertical position and made of a 6-mm-o.d. Pyrex glass tube, and the catalyst was held between two layers of quartz wool. The quantity of catalyst (5 to 20 mg) was adjusted to assure that highly active catalysts yielded low conversions (below 5%). The gas mixture, $CH_3OH/O_2/He=6/11/83$ (mol%), flowed from the top to the bottom of the reactor, and the reaction products were analyzed by an on-line gas chromatograph (GC) (HP 5840 A) containing two columns (Porapak R and Carbosieve SII) with two detectors (FID and TCD). The catalytic activity (TON) was calculated from the moles of methanol converted per mole of surface rhenium atom per second after correcting for the reactivity of support.

RESULTS AND DISCUSSION

Raman Spectroscopy: Ambient Conditions

The Raman spectra of 1% Re_2O_7 supported on ZrO_2 and TiO_2 under ambient conditions, where the catalysts possess adsorbed moisture (26), are shown in Fig. 1. The strong Raman features of ZrO_2 and TiO_2 below 700 cm^{-1} prevent acquisition of the diagnostic Raman bands for other rhenate functionalities (the bending mode of the $Re-O-Re$ linkage is found at $\sim 200\text{ cm}^{-1}$). The 1% Re_2O_7/ZrO_2 catalyst exhibits Raman bands at 968, ~ 930 , and 754 cm^{-1} . The band observed at 968 cm^{-1} is assigned to the symmetric stretching mode of terminal $Re=O$ of the surface rhenium oxide species on ZrO_2 (14, 15). The origin of the band at

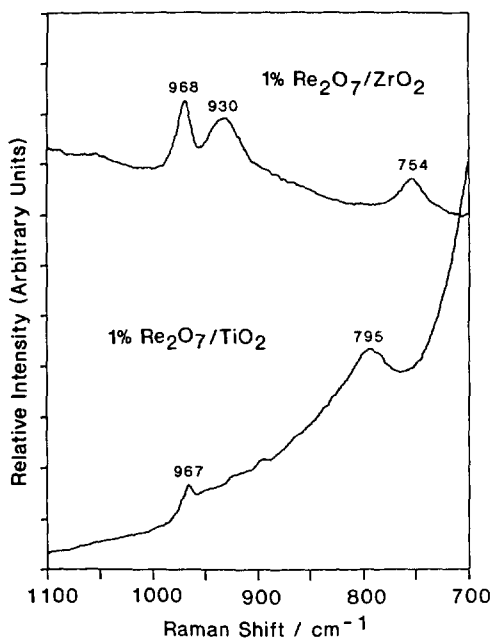


FIG. 1. Raman spectra of 1% Re_2O_7 supported on ZrO_2 and TiO_2 under ambient conditions.

$\sim 930\text{ cm}^{-1}$ is not entirely clear, but it may be associated with impurities in ZrO_2 (Cl and F) because this band is not present as the rhenium oxide content increases (13). The asymmetric $Re=O$ stretching mode of the surface rhenium oxide species overlaps with the $\sim 930\text{ cm}^{-1}$ band. The band observed at 754 cm^{-1} originates from the ZrO_2 support. The 1% Re_2O_7/TiO_2 catalyst possesses a Raman band for the symmetric stretching mode of the surface rhenium oxide species at 967 cm^{-1} . The band at 795 cm^{-1} originates from the first overtone of the 395 cm^{-1} band of TiO_2 (anatase). The asymmetric mode of the surface rhenium oxide species on TiO_2 was not obtained because of the strong TiO_2 background and the weak rhenium oxide signal.

The Raman spectra of 1% Re_2O_7 supported on Al_2O_3 and MgO under ambient conditions are presented in Fig. 2. The 1% Re_2O_7/Al_2O_3 catalysts exhibit Raman bands at 970 cm^{-1} ($\nu_s(Re=O)$), $\sim 919\text{ cm}^{-1}$ ($\nu_{as}(Re=O)$), and 332 cm^{-1} ($\delta(O=Re=O)$) for the surface

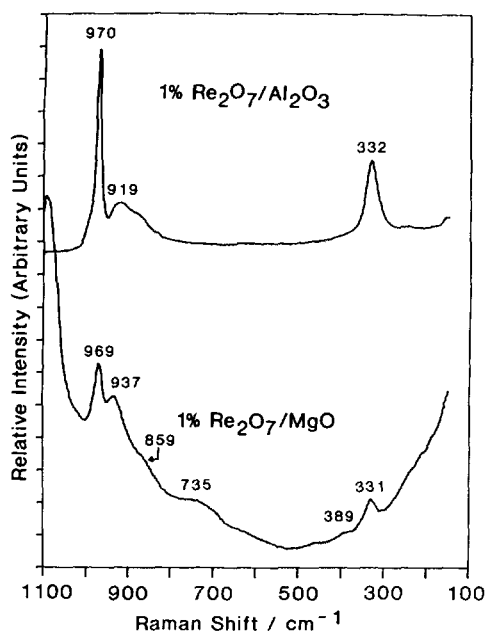


FIG. 2. Raman spectra of 1% Re_2O_7 supported on Al_2O_3 and MgO under ambient conditions.

rhenum oxide species (13, 15). The Raman spectrum of 1% $\text{Re}_2\text{O}_7/\text{MgO}$ exhibits Raman bands at 969 and 331 cm^{-1} , which are assigned to the symmetric ($\nu_s(\text{Re}=\text{O})$) and bending ($\delta(\text{O}=\text{Re}=\text{O})$) modes of surface rhenum oxide species. The asymmetric band of the $\text{Re}=\text{O}$ bond overlaps with the $\sim 937 \text{ cm}^{-1}$ band. The weak Raman bands observed at ~ 937 , ~ 859 , ~ 735 , and $\sim 389 \text{ cm}^{-1}$ are attributed to the mixed oxides formed by strong acid–base interaction of ReO_4^- with MgO (see discussion below).

The Raman spectrum of the 1% $\text{Re}_2\text{O}_7/\text{SiO}_2$ catalyst was not obtainable because of the strong fluorescence from the background of the $\text{Re}_2\text{O}_7/\text{SiO}_2$ catalyst. The fluorescence derived from the $\text{Re}_2\text{O}_7/\text{SiO}_2$ catalyst can be removed by the high-temperature precalcination (873–973 K). However, the surface rhenum oxide species on SiO_2 is not stable at elevated temperature and is volatile during high temperature precalcination.

The Raman spectra of 1% $\text{Re}_2\text{O}_7/\text{support}$

(ZrO_2 , TiO_2 , Al_2O_3 , and MgO) under ambient conditions show that only one type of rhenum oxide species is present on the support surface. The band position of the symmetric stretching mode of the terminal $\text{Re}=\text{O}$ bond for the 1% $\text{Re}_2\text{O}_7/\text{support}$ samples ($967\text{--}970 \text{ cm}^{-1}$) is similar to that of the ReO_4^- species (971 cm^{-1}), which is observed in an aqueous solution (12, 15). Similar observations are made for the supported V_2O_5 , MoO_3 , and CrO_3 catalysts under ambient conditions. Under ambient conditions, the adsorbed water hydrolyzes the bridging oxygen interacting with the support (metal–O–support bond), and the surface metal oxide species on the oxide supports is essentially in an aqueous medium (13, 15, 26). Although the Raman spectrum for the 1% $\text{Re}_2\text{O}_7/\text{SiO}_2$ catalyst could not be obtained in this investigation, the ReO_4^- species should be the only species present on SiO_2 since the ReO_4^- species is the only species that exists in aqueous solution (15, 28). Furthermore, at high rhenum oxide loadings, the Raman band can be observed and does occur at 971 cm^{-1} (13) consistent with the above model. The 1% $\text{Re}_2\text{O}_7/\text{MgO}$ catalyst also possesses a solid-solution formed by a strong acid–base reaction of rhenum oxide with MgO (see discussion below) in addition to the ReO_4^- species.

Raman Spectroscopy:

Dehydrated Conditions

The Raman spectra of 1% Re_2O_7 supported on ZrO_2 and TiO_2 under dehydrated conditions, where adsorbed water is desorbed, are shown in Fig. 3. The strong Raman features due to the ZrO_2 and TiO_2 supports limit the collection of the data below 700 cm^{-1} . The 1% $\text{Re}_2\text{O}_7/\text{ZrO}_2$ catalyst possesses Raman bands at 990, 884, and 754 cm^{-1} . The bands at 990 and 884 cm^{-1} are assigned to the symmetric and asymmetric stretching mode of the terminal $\text{Re}=\text{O}$ of the dehydrated surface rhenum oxide species on ZrO_2 , respectively (13, 15). The band observed at 754 cm^{-1} is due to the ZrO_2 support. The 1% $\text{Re}_2\text{O}_7/\text{TiO}_2$ catalyst

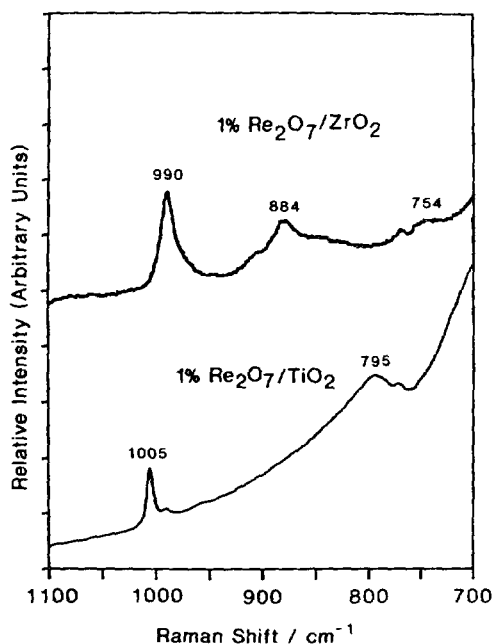


FIG. 3. Raman spectra of 1% Re₂O₇ supported on ZrO₂ and TiO₂ under dehydrated conditions.

exhibits Raman bands at 1005, ~980, and 795 cm⁻¹. The bands at 1005 and ~980 cm⁻¹ are attributed to the symmetric and asymmetric stretching mode of terminal Re=O of the dehydrated surface rhenium oxide species on TiO₂, respectively. The band at 795 cm⁻¹ originates from the anatase phase of TiO₂.

The Raman spectra of 1% Re₂O₇ on Al₂O₃ and MgO under dehydrated conditions are presented in Fig. 4. The 1% Re₂O₇/Al₂O₃ catalyst exhibits Raman bands at 1000, 878, and ~339 cm⁻¹, which are assigned to the symmetric, asymmetric stretching, and bending modes of the dehydrated surface rhenium oxide species on Al₂O₃, respectively (12, 13, 15). The weak shoulder observed in the spectrum at ~460 cm⁻¹ is attributed to the detector noise or the alumina support (13). The Raman spectrum of the 1% Re₂O₇/MgO catalyst shows different Raman characteristics compared to the other supported rhenium oxide catalysts. The 1% Re₂O₇/MgO catalyst possesses very strong

Raman bands at 943, 926, and 887 cm⁻¹ and weak bands at 771 and 381 cm⁻¹. The very different Raman features for the Re₂O₇/MgO catalyst appears to be due to the formation of a new phase, Re₂O₇-MgO mixed oxides (see discussion below).

The dehydrated Raman spectrum for the 1% Re₂O₇/SiO₂ catalyst was not obtainable due to the reasons previously stated. Previous studies reveal that silica-supported MoO₃ (33), V₂O₅ (34), and CrO₃ (35) possess isolated surface molybdenum, vanadium, and chromium oxide species, respectively, on silica, regardless of the MoO₃, V₂O₅, and CrO₃ content. This is attributed to the extremely low surface OH density of SiO₂ (36). Vuurman *et al.* (13) have reported that the dehydrated 4.4 and 5.2% Re₂O₇/SiO₂ catalysts possess isolated, four-coordinated surface rhenium oxide species with three terminal Re=O bands and one bridging Re-O-Si bond ($\nu_s = 1015$ cm⁻¹, $\nu_{as} = 975$ cm⁻¹). Therefore, the surface rhenium oxide species for the 1% Re₂O₇/SiO₂ catalyst is

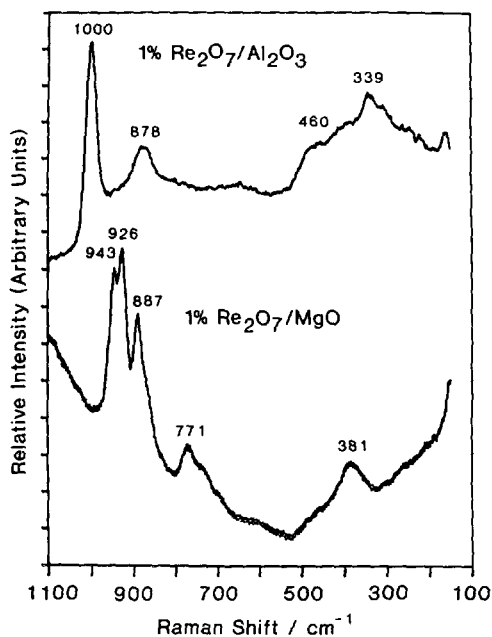


FIG. 4. Raman spectra of 1% Re₂O₇ supported on Al₂O₃ and MgO under dehydrated conditions.

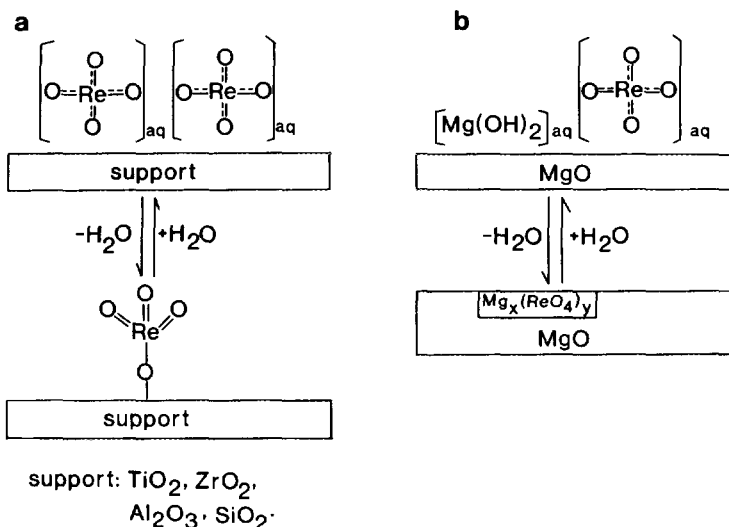
not expected to be very different from that of 4.4 and 5.2% $\text{Re}_2\text{O}_7/\text{SiO}_2$ catalysts.

The Raman spectra of the 1% $\text{Re}_2\text{O}_7/\text{support}$ catalysts under dehydrated conditions suggest that the same type of surface rhenium oxide species is present on the different oxide supports at low loadings with the exception of the MgO support. The absence of characteristic Raman features due to the Re—O—Re linkages at $\sim 200\text{ cm}^{-1}$ for the 1% $\text{Re}_2\text{O}_7/\text{Al}_2\text{O}_3$ sample, indicates that the surface rhenium oxide species appears to be isolated on the oxide support surface. The position of the symmetric stretching mode of Re=O ($990\text{--}1005\text{ cm}^{-1}$) for the 1% $\text{Re}_2\text{O}_7/\text{support}$ catalysts is much higher than that for octahedrally coordinated rhenium oxide, which is observed for $\alpha\text{-Li}_6\text{ReO}_6$ (680 cm^{-1}) (29), and *in situ* XANES studies possess a strong pre-edge feature consistent with four-coordinated rhenium oxide species (15). The band position is much lower than that of ReF_3O_2 (C_{2v} , 1026 cm^{-1}) (30) and much higher than that of ReO_4^- (aq) (T_d , 971 cm^{-1}) (28) and NaReO_4 (S_4 , 963 cm^{-1}) (31). The band position for the dehydrated 1% $\text{Re}_2\text{O}_7/\text{support}$ catalysts, however, falls in the region observed for ReO_3F (C_{3v} , $\nu_s = 1009\text{ cm}^{-1}$), ReO_3Cl (C_{3v} , $\nu_s = 1001\text{ cm}^{-1}$), or ReO_3Br (C_{3v} , $\nu_s = 997\text{ cm}^{-1}$) species, which possess three terminal Re=O bonds and one Re—O—Z (Z=F, Cl, Br) bond (32). Therefore, the structure of the surface rhenium oxide is essentially independent of the type of support, with the exception of MgO, and possesses isolated, four-coordinated surface rhenium oxide species with three terminal Re=O bonds and one bridging Re—O—support bond.

The dehydrated Raman band position of the symmetric Re=O stretch for the surface rhenium oxide species varies with the type of oxide support and decreases in the order: SiO_2 (1015 cm^{-1}) (13) > TiO_2 (1005 cm^{-1}) > Al_2O_3 (1000 cm^{-1}) > ZrO_2 (990 cm^{-1}) (see Figs. 3 and 4). Consequently, the surface rhenium oxide species on SiO_2 possesses the shortest Re=O bond and the surface rhenium oxide species on ZrO_2 possesses

the longest Re=O bond. A similar observation has been made for the 1% $\text{V}_2\text{O}_5/\text{support}$ (SiO_2 , Nb_2O_5 , TiO_2 , Al_2O_3 , and ZrO_2) system (18). These results indicate that the physical characteristics of the surface metal oxide species are influenced by the specific oxide support. Eischen and Pliskin (37) have demonstrated that the adsorption of CO on supported metals on oxide supports possesses different coordination numbers (atop, bridge, or hollow sites), which results in slight shifts in the band position of $\text{C}\equiv\text{O}$ bond. Hulse and Moskovits (38) have also revealed that the IR band position of the $\text{C}\equiv\text{O}$ bond on Ni is dependent on the number of nickel atoms that are bonded to $\text{C}\equiv\text{O}$ and decreases as the number of nickel atoms increases. It is well established that different oxide supports possess different average coordination numbers of oxygen anions, and the average coordination number of oxygen anions for SiO_2 , TiO_2 , Al_2O_3 , and ZrO_2 is 2, 3, 3–4, and 3–4, respectively (39, 40). Therefore, the shift in Raman band position for the 1% Re_2O_7 on different oxide supports is believed to be related to the different coordination numbers of the oxygen anions in the oxide supports. The slightly lower Raman band position of the zirconia sample relative to the alumina sample may be due to impurities in the zirconia system.

The symmetric stretching mode of the terminal rhenium–oxygen bond for the $\text{Re}_2\text{O}_7/\text{support}$ catalysts (ZrO_2 , TiO_2 , SiO_2 , and Al_2O_3) under ambient conditions ($967\text{--}970\text{ cm}^{-1}$) generally shifts to higher wavenumber ($990\text{--}1005\text{ cm}^{-1}$) upon dehydration due to the further distortion caused by the direct interaction with the support and formation of true terminal bonds (13). However, for the 1% $\text{Re}_2\text{O}_7/\text{MgO}$ catalyst, the Raman bands behave differently. This observation suggests a different type of interaction between rhenium oxide and MgO. Knozinger and co-workers (41) found the formation of a bulk compound, i.e., anhydrous $\text{Mg}(\text{ReO}_4)_2$, for high loadings of $\text{Re}_2\text{O}_7/\text{MgO}$ (20 wt% Re), the anhydrous $\text{Mg}(\text{ReO}_4)_2$ being sensitive to hydration and dehydration



SCHEME 1. Two-dimensional model of the supported 1% Re_2O_7 catalysts under ambient and dehydrated conditions.

effects. Wang (12) has demonstrated that MgO is readily soluble in water and easily makes a compound with ReO_4^- (aq) during aqueous preparation, which suggests that the formation of surface rhenium oxide species on MgO is not favored. The Raman band positions for 1% $\text{Re}_2\text{O}_7/\text{MgO}$ in the present study do not correspond with the Raman bands of crystalline $\text{Mg}(\text{ReO}_4)_2$; however, the very different behavior of the $\text{Re}_2\text{O}_7/\text{MgO}$ system and the previous studies (12, 41) suggest the formation of mixed oxides as a major component.

The proposed surface structures for 1% rhenium oxide on the different oxide supports (TiO_2 , ZrO_2 , Al_2O_3 , SiO_2 , and MgO) are presented in Scheme 1. Under ambient conditions, the surface rhenium oxide species are hydrated by adsorbed moisture and are essentially in an aqueous medium. Deo and Wachs (26) have proposed that the molecular structures of surface metal oxide species on different oxide support (Al_2O_3 , TiO_2 , ZrO_2 , SiO_2 , and MgO) under ambient conditions are dependent on the net pH at which the surface possesses zero surface charge (point of zero charge). The surface pH at PZC is determined by the specific

oxide support and surface coverage of the metal oxide overlayer. ReO_4^- is the only stable species in an aqueous solution regardless of pH or concentration (26) and consequently, only the ReO_4^- species is present on the hydrated surfaces of the different 1% $\text{Re}_2\text{O}_7/\text{support}$ catalysts. The adsorbed water molecules readily desorb at elevated temperature and the surface rhenium oxide species anchor to the oxide support by forming an oxygen bridge with the oxide support. The Raman spectroscopic studies under dehydrated conditions show that the molecular structures of the dehydrated surface rhenium oxide species supported on the different oxide supports (TiO_2 , ZrO_2 , SiO_2 , and Al_2O_3) possess an isolated, four-coordinated rhenium oxide species with three terminal $\text{Re}=\text{O}$ bonds and one bridging $\text{Re}-\text{O}-\text{support}$ bond regardless of type of oxide support (see Scheme 1a). Similar observations were also found for $\text{Re}_2\text{O}_7/\text{Nb}_2\text{O}_5$ catalysts (42). The rhenium oxide species in the $\text{Re}_2\text{O}_7/\text{MgO}$ catalyst shows quite different characteristics compared to the other oxide supports. The hydrated rhenium oxide species, ReO_4^- , is also present on the MgO surface under ambient conditions. In

TABLE I
Catalytic Activity for the Methanol Oxidation over
1% Re₂O₇/Support Catalysts^a

Support	Total rate (mmol g ⁻¹ h ⁻¹)	TON (s ⁻¹)	T _{max} (K) ^b
TiO ₂	178.3	1.2 × 10 ⁰	490
ZrO ₂	25.6	1.7 × 10 ⁻¹	570
SiO ₂	3.0	2.0 × 10 ⁻²	580
MgO	0	0	693 ^c
Al ₂ O ₃	0	0	710

^a Reaction temperature is 503 K; CH₃OH/O₂/He=6/11/83 (mol%). Corrected for reactivity due to the oxide support itself.

^b Maximum temperature of reaction, from Ref. (13).

^c Reference (12).

addition, MgO is readily soluble in water and forms Mg(OH)₂ under ambient conditions. This hydroxide probably exists as a thin film covering the MgO support under ambient conditions. Upon dehydration, the adsorbed water molecules are desorbed at elevated temperature and the rhenium oxide species appears to form a mixed oxide, such as Mg_x(ReO₄)_y (Scheme 1b). This mixed oxide phase is probably present as a thin metal oxide film since it can be hydrated by adsorbed moisture under ambient conditions.

Methanol Oxidation

The turnover number (TON) for methanol oxidation over 1% Re₂O₇ on the different oxide supports (TiO₂, ZrO₂, SiO₂, MgO, and Al₂O₃) is shown in Table I. The catalytic activity (overall rate) of the pure TiO₂, ZrO₂, SiO₂, and MgO supports are 2.3, 7.3, 1.0, 8.4 mmol g⁻¹ h⁻¹, respectively. The pure Al₂O₃ support showed a very high activity (100 mmol g⁻¹ h⁻¹) for methanol dehydration and 100% selectivity toward CH₃OCH₃, which is related to the surface Lewis acid sites (43). The catalysts used in this study contain only 1% rhenium oxide by weight so that a large portion of the oxide support surface is exposed for these catalysts. Therefore, the TON for methanol oxidation over 1% Re₂O₇/support was obtained

by correcting the reactivity due to the support itself. The TON varies with the type of oxide support as presented in Table I. The 1% Re₂O₇/TiO₂ catalyst is the most active for methanol oxidation and this value is at least 1–2 orders of magnitude higher than that of the other catalysts. The 1% Re₂O₇/Al₂O₃ catalyst does not show any reactivity due to the surface rhenium oxide species. Similarly, the 1% Re₂O₇/MgO is also inert for methanol oxidation. The TON for methanol oxidation over the different 1% Re₂O₇/support catalysts is strongly dependent on the type of oxide support and decreases in the order: TiO₂ > ZrO₂ > SiO₂ > MgO ≈ Al₂O₃. As shown in Table I, the reducibility of the rhenium oxide species in TPR experiments is also found to vary with the nature of the oxide support. The reducibility of the 1% Re₂O₇/support decreases in the order: TiO₂ > ZrO₂ ≥ SiO₂ > MgO ≥ Al₂O₃. Thus, the TON for methanol oxidation correlates with the reducibility of supported rhenium oxide catalysts. The Re₂O₇/ZrO₂ and Re₂O₇/SiO₂ catalysts possess somewhat similar reducibility, but the activity for methanol oxidation over Re₂O₇/SiO₂ is 1 order of magnitude lower than the Re₂O₇/ZrO₂ catalyst. This result is attributed to the volatility of surface rhenium oxide species on SiO₂ during the methanol oxidation since Re₂O₇ deposits (light yellow) were found on the walls downstream of the reactor. Recent studies of a series of Re₂O₇/TiO₂ catalysts indicate that the turnover number is independent of rhenium oxide loading (19), which overcomes the effect of using different surface areas for the oxide supports.

The product selectivity for methanol oxidation over the 1% Re₂O₇/support catalysts is listed in Table 2. The main reaction product for 1% Re₂O₇/TiO₂ is formaldehyde (HCHO), and methyl formate (HCOOCH₃) is next in abundance. For the 1% Re₂O₇/ZrO₂, HCOOCH₃ is the major reaction product, and HCHO and combustion products such as CO/CO₂ are next in abundance. The high selectivity for HCOOCH₃ over 1% Re₂O₇/ZrO₂ catalysts is attributed to the

TABLE 2
 Selectivity for the Methanol Oxidation over 1% Re₂O₇/Support Catalysts^a

Support	Selectivity				
	HCHO	HCOOCH ₃	(CH ₃ O) ₂ CH ₂	CH ₃ OCH ₃	CO + CO ₂
TiO ₂	68.2	24.0	1.2	0.9	5.7
ZrO ₂	21.4	62.3	0	2.4	13.9
SiO ₂	9.8	0	0	1.0	89.2
MgO ^b	21.4	0	0	0	78.6
Al ₂ O ₃ ^b	0	0	0	100.0	0

^a Reaction temperature is 503 K; CH₃OH/O₂/He=6/11/83 (mol%).

^b The selectivity is only attributed to the support itself.

high activity and selectivity for HCOOCH₃ of the ZrO₂ support. The 1% Re₂O₇/SiO₂ catalyst gives CO/CO₂ and HCHO. A large portion of the CO/CO₂ is due to the SiO₂ support because the SiO₂ support itself shows 100% selectivity toward CO/CO₂. The 1% Re₂O₇/Al₂O₃ exhibits 100% dimethyl ether (CH₃OCH₃), which is due to the acidic properties of the Al₂O₃ support itself (43). The absence of redox products (HCHO or HCOOCH₃) reveals that the surface rhenium oxide species are not very active on Al₂O₃. The 1% Re₂O₇/MgO catalyst yields CO/CO₂ combustion products and HCHO, which are due to the MgO support itself. The result indicates that the distribution of reaction products can also be influenced by the specific oxide support.

The present Raman data of the different 1% Re₂O₇/support catalysts reveal that the four-coordinated, dehydrated surface rhenium oxide species is present on all the oxide supports, with the exception of the 1% Re₂O₇/MgO catalyst. The activation energy measured for methanol oxidation over 1% Re₂O₇ supported on TiO₂, ZrO₂, and SiO₂ is similar regardless of the type of oxide support (21.7 ± 1.0 kcal mol⁻¹). The activation energy for methanol oxidation over 1% Re₂O₇ supported on Al₂O₃ and MgO is not measurable because of the very low activity of the surface rhenium oxide species on these catalysts. A similar activation energy for methanol oxidation is observed for sup-

ported 1% V₂O₅ catalysts (18.3 ± 0.9 kcal mol⁻¹) regardless of the type of oxide support (18). It is well established that the C-H bond cleavage in adsorbed CH₃O on MoO₃ (44) and MoO₃/SiO₂ (45) is the rate-determining step in the methanol oxidation from isotopic studies. The activation energy of 1% Re₂O₇/support is similar to the value for the breaking of the C-H bonds of CH₃O adsorbed species on MoO₃ (20.6 kcal mol⁻¹) (44). The present results indicate that the methanol oxidation reaction over supported surface rhenium oxide species possesses the same rate-determining step. It should be noted that from thermogravimetry experiments the moisture formed during reaction does not appear to coordinate with the surface rhenium oxide species.

The same surface rhenium oxide species with the same rate-determining step, however, exhibits significantly different catalytic activities for methanol oxidation. In addition, the catalytic activity for methanol oxidation correlates with the reducibility of surface rhenium oxide species on different oxide supports. A similar trend is observed for the V₂O₅/support (18, 19, 25) and MoO₃/support systems (19). These results indicate that the reactivity for methanol oxidation is dependent on the specific oxide support and also on the specific surface metal oxide species.

The above results suggest that the number of active sites and/or activity per site during

methanol oxidation over supported rhenium oxide catalysts depends on the type of oxide support. The number of catalytic active sites and/or number of active sites is strongly dependent on the reducibility of the surface rhenium oxide species, which is influenced by the different surface rhenium oxide-support interactions ($\text{Re}^{7+}\text{-O}\text{-support}$). It is well known that the primary step in methanol oxidation is a dissociative adsorption of CH_3OH on the supported (46) and unsupported metal oxides (47), which result in the formation of adsorbed CH_3O and hydroxyls. Formaldehyde and the other partial oxidation products are then formed from the surface CH_3O species. The role of the $\text{Re}^{7+}\text{-O}\text{-support}$ bond in the formation of the surface CH_3O and HCHO is presently not clear. Experiments are currently underway to elucidate the connection between the $\text{Re}^{7+}\text{-O}\text{-support}$ bond and the number of active sites and/or activity per site.

The different selectivity for methanol oxidation over the 1% $\text{Re}_2\text{O}_7/\text{support}$ catalysts is attributed to the surface chemistry contribution of the oxide supports because TiO_2 , ZrO_2 , Al_2O_3 , SiO_2 , and MgO supports are active for the conversion of methanol to HCOOCH_3 , CH_3OCH_3 , CO/CO_2 , HCHO , and CO/CO_2 , respectively.

CONCLUSIONS

The surface rhenium oxide species for 1% Re_2O_7 on different oxide supports (ZrO_2 , TiO_2 , SiO_2 , Al_2O_3 , and MgO), under ambient conditions, resembles the ReO_4^- species present in an aqueous solution. Under dehydrated conditions, the surface rhenium oxide species possesses isolated and four-coordinated rhenium oxide species with three terminal $\text{Re}=\text{O}$ and one bridging $\text{Re}-\text{O}$ -support bond. For the 1% $\text{Re}_2\text{O}_7/\text{MgO}$ catalyst under dehydrated conditions, a mixed oxide such as $\text{Mg}_x(\text{ReO}_4)_y$ appears to be present on MgO . The methanol oxidation studies reveal that the supported rhenium oxide catalysts possess the same activation energy, but the activity varies significantly. The differences in the activity are attributed

to the differences in the surface rhenium oxide-support interaction, since the same surface rhenium oxide species are present on the different supports (with the exception of $\text{Re}_2\text{O}_7/\text{MgO}$). Moreover, the increase in activity for methanol oxidation with increasing reducibility of the surface rhenium oxide species suggests that a decrease in $\text{Re}^{7+}\text{-O}\text{-support}$ bond strength results in an increase in the number of catalytic active sites and/or the activity per site.

REFERENCES

1. Moulijn, J. A., and Mol, J. C., *J. Mol. Catal.* **46**, 1 (1988); Mol, J. C., and Moulijn, J. A., "Advances in Catalysis" (D. D. Eley, H. Pines, and P. B. Weisz, Eds.), Vol. 24, p. 131. Academic Press, New York, 1975.
2. Olsthoorn, A. A., and Boelhouwer, C., *J. Catal.* **44**, 207 (1976).
3. Pecoraro, T. A., and Chianelli, R. R., *J. Catal.* **67**, 430 (1981).
4. Thomas, R., Van Oers, E. M., De Beer, V. H. J., Medema, J., and Moulijn, J. A., *J. Catal.* **76**, 241 (1982).
5. Nakamura, R., and Echigoya, E., *Recl. Trav. Chim. Pays Bas* **96**, M31 (1977).
6. Xiaoding, X., Imhoff, P., Van Den Aarweg, G. C. N., and Mol, J. C., *J. Chem. Soc. Chem. Commun.* 273 (1985).
7. Xiaoding, X., and Mol, J. C., *J. Chem. Soc. Chem. Commun.*, 631 (1985).
8. Mol, J. C., and Andreini, A., *J. Mol. Catal.* **46**, 131 (1988).
9. Andreini, A., Xiaoding, X., and Mol, J. C., *Appl. Catal.* **46**, 131 (1988).
10. Xiaoding, X., Boelhouwer, C., Benecke, J. I., Vonk, D., and Mol, J. C., *J. Chem. Soc. Faraday Trans. 1* **82**, 1945 (1986).
11. Nakamura, R., Abe, F., and Echigoya, E., *Chem. Lett. Jpn. Chem. Soc.*, 51 (1981).
12. Wang, L., Ph.D. thesis, University of Wisconsin, 1982; Wang, L., and Hall, K. E., *J. Catal.* **82**, 177 (1983).
13. Vuurman, M. A., Wachs, I. E., Stufkens, D. J., and Oskam, A., *J. Mol. Catal.* **76**, 263 (1992).
14. Ellison, A., Diakun, G., and Worthington, P., *J. Mol. Catal.* **46**, 131 (1988).
15. Hardcastle, F. D., and Wachs, I. E., Horsley, J. A., and Via, G. H., *J. Mol. Catal.* **46**, 15 (1988).
16. Kerkhof, F. P. J. M., Moulijn, J. A., and Thomas, R., *J. Catal.* **56**, 279 (1979).
17. Williams, K. P. J., and Harrison, K., *J. Chem. Soc. Faraday Trans.* **86**, 1603 (1990).
18. Deo, G., and Wachs, I. E., *J. Catal.* **129**, 307 (1991).
19. Wachs, I. E., Deo, G., Kim, D. S., Vuurman,

- M. A., and Hu, H., in "Proceedings, 10th International Congress on Catalysis, Budapest, 1992" (L. Guzzi, Ed.), Preprint and abstract book p. 72. Institute of Isotopes of the Hungarian Academy of Sciences, Budapest, 1992.
20. Arnoldy, P., Van Oers, E. M., Bruinsma, O. S. L., De Beer, V. H. J., and Moulijn, J. A., *J. Catal.* **93**, 231 (1985).
21. Tatibouet, J. M., Germain, J. E., and Votla, J. C., *J. Catal.* **82**, 240 (1983).
22. Ohuchi, F., Firment, L. E., Chowdhry, U., and Ferretti, A., *J. Vac. Sci. Technol. A* **2**, 1022 (1984).
23. Louis, C., Tatibouet, J. M., and Che, M., *J. Catal.* **109**, 354 (1988).
24. Segawa, K., Soeya, T., and Kim, D. S., *Sekiya Gakkaishi (J. Jpn. Petrol. Inst.)* **33**, 347 (1990).
25. Roozeboom, F., Cordingley, P. D., and Gellings, P. J., *J. Catal.* **68**, 464 (1981).
26. Deo, G., and Wachs, I. E., *J. Phys. Chem.* **95**, 5889 (1991).
27. Parks, G. A., *Chem. Rev.* **65**, 177 (1965).
28. Gonzalez-Vichez, F., and Griffith, J. *Chem. Soc. Dalton Trans.* 1416 (1972).
29. Hauch, J., and Fadini, A., *Z. Naturforsch* **256**, 422 (1970).
30. Beattie, I. R., Crocombe, R. A., and Ogden, J. S., *J. Chem. Soc. Dalton Trans.* 1481 (1972).
31. Johnson, R. A., Rogers, M. T., and Leroi, G. E., *J. Chem. Phys.* **56**, 789 (1972).
32. Muller, A., Krebs, B., and Holtje, W., *Spectrochim. Acta* **23**, 2753 (1967).
33. Hu, H., and Wachs, I. E., unpublished work.
34. Deo, G., Ph.D. thesis, Lehigh University, 1992.
35. Kim, D. S., Tatibouet, J. M., and Wachs, I. E., *J. Catal.* **136**, 209 (1992).
36. Kim, D. S., Segawa, K., Soeya, T., and Wachs, I. E., *J. Catal.*, in press.
37. Eischen, R. P., and Pliskin, W. A., in "Advances in Catalysis" (D. D. Eley, W. G. Frankenburg, and V. I. Komarewsky, Eds.), Vol. 10, p. 1. Academic Press, New York, 1958.
38. Hulse, J. E., and Moskovits, M., *Surf. Sci.* **57**, 125 (1976).
39. Boehm, H. P., and Knozinger, H., in "Catalysis: Science and Technology" (J. R. Anderson and M. Boudart, Eds.), Vol. 4, p. 39. Springer-Verlag, Berlin/Heidelberg, 1983.
40. Ikeya, T., and Senna, M., *J. Non-Cryst. Solids* **105**, 243 (1988).
41. Gazzoli, D., Valigi, M., Vielhaber, B., and Knozinger, H., *J. Less-Common Met.* **134**, 67 (1987).
42. Jehng, J. M., and Wachs, I. E., *Appl. Catal. A* **83**, 179 (1992).
43. Jehng, J. M., and Wachs, I. E., *Catal. Today* **8**, 37 (1990).
44. Fareneth, W. E., Ohuchi, F., Staley, R. H., Chowdhry, U., and Sleight, A. W., *J. Phys. Chem.* **89**, 2493 (1985).
45. Yang, T. J., and Lunsford, J. H., *J. Catal.* **103**, 55 (1987).
46. Busca, G., *J. Mol. Catal.* **50**, 241 (1989).
47. Morrow, B. A., *J. Chem. Soc. Faraday, Trans. 1* **70**, 1527 (1974).